Bending Analysis of Steel-Concrete Composite Beams with Porosity

Prashant Kumar
Department of Civil Engineering, National Institute of Technology Patna, India
pk0895300@gmail.com (corresponding author)

Ajay Kumar
Department of Civil Engineering, National Institute of Technology Delhi, India
sajaydce@gmail.com

Received: 17 May 2023 | Revised: 26 May 2023 | Accepted: 28 May 2023

 DOI: https://doi.org/10.48084/etasr.6050

ABSTRACT

This study investigated the bending behavior of a simply supported pervious composite beam using the finite element method based on cubic order beam theory. The cubic order axial displacement was assumed and solved using shear stress-free conditions on the extreme surfaces of the composite beam. For simplicity, this study considered one-dimensional axial displacement. Three nodded finite elements were assumed, and each node had eight unknowns. Shear locking was eliminated in the present model by numerical integration of the stiffness matrix. A uniform porosity distribution was implemented in the upper layer of the composite beam. The damping ratio was also considered for the bending analysis. The accuracy of the present model makes it robust for the analysis of composite beams.

Keywords- porous concrete; finite element method; bending response; shear interface; shear stress

I. INTRODUCTION

Lightweight materials with higher strength are always the first choice of engineers. Composite materials meet all the criteria for complex construction. Over the past forty years, high-temperature resistant, more flexible, high-strength, and cost-effective composite materials have been created for civil engineering, aerospace technology, and the formation of household materials. Other applications for these materials include electrical appliances, energy transformation, biomedical engineering, optics, etc. [1-2]. The advantages of these structures are their high strength, improved material properties, and lower weight.

Functionally graded composites can fulfill current and distinctive functions that traditional composite materials cannot [3]. These are sophisticated composite materials with a microscopically inhomogeneous morphology that are created using powder metallurgy processes from a combination of metal and ceramic. There are fewer stress discontinuities in FG materials because the material characteristics change gradually and smoothly across the thickness, and interlaminar stress discontinuities are removed. Knowing the bending, buckling, and free vibration frequencies is vital because structural components made of composite laminates, such as aircraft wings and panels, are regularly subjected to mechanical loads, critical buckling, shocks, and vibrations [4].

The static and dynamic analysis of beams has an exciting history for its development. Various beam theories have been developed to get precise and accurate results. The Euler-Bernoulli beam theory is used to analyze the beam [5]. As the Euler-Bernoulli beam theory is not enough to analyze a thin beam, the Timoshenko Beam Theory (TBT) has become popular [6-7]. High-order Beam Theory (HBT) is more accurate than TBT. Today, HBT is the first choice for the analysis of beam behavior [8-10].

The strength of a composite material also depends on the type and strength of shear studs used to hold the two elements, so investigation of shear stiffness parameters and inter-layer slip is essential [11-12]. In [13-15], the impact of porosity distribution on the vibrational behavior was investigated. In [16], the dynamic behavior of a beam was examined under various loading conditions using the state-space technique.

This study investigated the impact of porosity distribution on the bending of simply supported two-layered sandwich steel-concrete composite beams. The one-dimensional C^0 finite element method was incorporated to model this problem and produce accurate results. The effect of the damping ratio was also calculated. To the best of our knowledge, the present work has not been used in any previous bending analysis study of composite beams. The novelty of the present work is the uniform distribution of porosity provided along the transverse direction of the upper element of the two-layered sandwich composite beam. The formation of voids at the time of modeling is a major issue for every engineer. So, its analysis is useful for future work.

II. FORMULATION

A. Porosity Distribution in the Upper Element

Porosity is incubated in the concrete element changing the material properties of the simply supported composite beam, such as Young's modulus (E), shear modulus (G), and density of the concrete element.

$$\begin{cases} E_c(y) = E_{cmax}(1-\kappa_c) \\ G_c(y) = G_{cmax}(1-\kappa_c) \\ \rho_c(y) = \rho_{cmax}\sqrt{1-e_{mc}\kappa_c} \end{cases} \quad (1)$$

where E is Young's modulus, G is the shear modulus, ρ is mass density, and k is the function of porosity.

B. Mathematical Formulation

The high-order beam theory was used to solve the cubic order axial displacement equation. Figure 1 shows the shear interface of the beam.

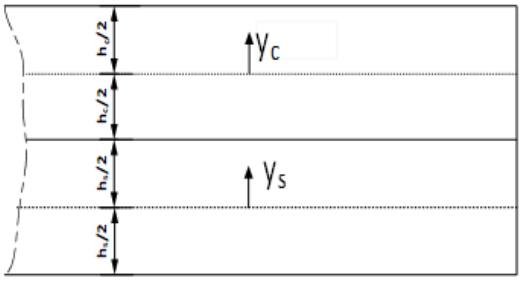

Fig. 1. Shear flexible interface of the composite beam.

The cubic order axial displacement equation for the upper and lower layer of the beam is written as:

$$[u_i] = [1 \quad -y_i \quad {y_i}^2 \quad {y_c}^3][u_{io} \quad \theta_i \quad \zeta_i \quad \xi_i]^T \quad (2)$$

where u is the axial displacement equation along the centroidal axis, θ is the bending rotation, ζ and ξ are higher order terms, and $I = c, s$. The transverse equation of both layers is expressed as:

$$W_c(x, y_c, z) = W_s(x, y_s, z) = W(x) = W \quad (3)$$

The partial shear interaction between two layers of the composite beam is modeled by taking distributed shear springs at their interface. Interfacial stiffness and shear slip at the interface are used to determine the shear stress at the interface. Interfacial slip (s) is calculated as given below, where u_c and u_s are the axial displacements of the upper and lower layer at the interface.

$$s = (u'_c - u'_s) \quad (4)$$

The axial displacements in (2) are higher-order equations that are concerned with the warping of the transverse sections but do not describe the commonly used displacement parameters adopted in beam theories. So, higher-order terms are eliminated using shear stress-free conditions at the extreme surfaces of the composite beam. The shear stress can be calculated at any point in the upper layer using (2) and (3).

$$[\tau_c] = [G_c][\gamma_c]$$

$$\gamma_c = \left\{\frac{\partial u_c}{\partial y_c} + \frac{\partial W}{\partial x}\right\}$$

$$= [-1 \quad 2y_c \quad 3{y_c}^2 \quad 1]\left[\theta_c \quad \zeta_c \quad \xi_c \quad \frac{\partial W}{\partial x}\right]^T \quad (5)$$

where γ_c is the shear strain and G_c is the shear modulus of the porous concrete layer.

$$\begin{aligned} A_c &= \left\{1 - \left(\frac{12y^2}{5{h_c}^2}\right) + \left(\frac{16y^3}{5{h_c}^3}\right)\right\}, \\ B_c &= \left\{\left(\frac{12y^2}{5{h_c}^2}\right) - \left(\frac{16y^3}{5{h_c}^3}\right)\right\}, \\ C_c &= \left\{-y - \left(\frac{4y^2}{5h_c}\right) + \left(\frac{12y^3}{5{h_c}^2}\right)\right\}, \\ D_c &= -\left\{\left(\frac{2y^2}{5h_c}\right) + \left(\frac{4y^3}{5{h_c}^2}\right)\right\} \\ A_s &= \left\{1 - \left(\frac{12y^2}{5{h_s}^2}\right) - \left(\frac{16y^3}{5{h_s}^3}\right)\right\}, \\ B_s &= \left\{\left(\frac{12y^2}{5{h_s}^2}\right) + \left(\frac{16y^3}{5{h_s}^3}\right)\right\}, \\ C_s &= \left\{-y + \left(\frac{4y^2}{5h_s}\right) + \left(\frac{12y^3}{5{h_s}^2}\right)\right\}, \\ D_s &= \left\{\left(\frac{2y^2}{5h_s}\right) - \left(\frac{4y^3}{5{h_s}^2}\right)\right\}, \text{ and } \chi = \frac{dW}{dx} \end{aligned} \quad (6)$$

The shear stress-free conditions are applied at the top and bottom surface of the beam to find out the displacement equation:

$$[u_i] = [A_i \quad B_i \quad c_i \quad D_i \quad][u_{io} \quad u_i \quad \theta_i \quad \chi]^T \quad (7)$$

The normal stress and normal strain at any point beam are calculated using the following equation:

$$\{\bar{\sigma}\}_j = [\bar{D}]_j\{\bar{\varepsilon}\}_j \quad (8)$$

where σ_j is the normal stress, τ_j is the shear stress, E_j is the modulus of elasticity, G_j is the shear modulus, ε_j is the normal strain, and γ_j is the shear strain of the j^{th} layer, and j=c represents the upper layer and j=s represents the lower layer of the two material composite beams.

$$\{\bar{\varepsilon}\}_j = \begin{Bmatrix} \varepsilon_j \\ \gamma_j \end{Bmatrix} = \begin{Bmatrix} \frac{\partial u_j}{\partial x} \\ \frac{\partial u_j}{\partial y_j} + \frac{\partial W}{\partial x} \end{Bmatrix} = [H]_j\{\varepsilon\}_j \quad (9)$$

The strain energy can be given as a function of stress and strain using (8) and (9):

$$u = \frac{1}{2}\int(\{\bar{\varepsilon}\}_c^T\{\bar{\sigma}\}_c + \{\bar{\varepsilon}\}_s^T\{\bar{\sigma}\}_s)dAdx$$

$$= \frac{1}{2}\int(\{\bar{\varepsilon}\}_c^T\{D\}_c\{\varepsilon\}_c + \{\bar{\varepsilon}\}_s^T\{D\}_s\{\varepsilon\}_s)dx \quad (10)$$

where:

$$[D]_c = \int[H]_c^T[\bar{D}]_c[H]_c dA_c \text{ and } [D]_s = \int[H]_s^T[\bar{D}]_s[H]_s dA_s$$

Numerical integration was used to evaluate the cross-section rigidity matrix $[D]_c$ and $[D]_s$. The stored strain energy was calculated using (4) and distributed shear springs stiffness k_s.

$$U = \frac{1}{2}\int k_s s^2 dx = \frac{1}{2}\int k_s(u_c - u_s)dx \quad (11)$$

C. Finite Element Formulation

Three nodded iso-parametric C^0 elements were selected. This theory assumed eight nodal degrees of freedom to solve the present problem using a one-dimensional finite element approximation. The unknown nodal displacement vector $\{d\}$ on the middle surface of a typical element is given by:

$$\{d\} = \sum_{i=1}^{3} \psi_i(x,y).\{d_i\} \quad (12)$$

where ψ_i is the shape function. The generalized strain vector as a function of the nodal displacement vector $\{d\}$ can be found by:

$$\{\varepsilon\}_j = \sum_{i=1}^{3} [P_i]\{d_i\} \quad (13)$$

where $[P_i]$ is the interpolation function differential operator matrix. The strain vectors were calculated using (11) and (13) as a function of the stiffness matrix $[K^l]$.

$$U = \frac{1}{2}\{d\}^T[K^l]\{d\} \quad (14)$$

where:

$$[K^l] = \int([P]_c^T[D]_c[P]_c + [P]_s^T[D]_s[P]_s)dx \quad (15)$$

Similarly, the interfacial stiffness and the stiffness due to the penalty function approach were calculated. An element's mass matrix and its geometric stiffness matrix can be found in the same way as the element stiffness matrix calculated above. Equations (3) and (12) were used to find the displacement component vector at a point in the beam layer as follows:

$$\{\bar{f}\} = \begin{Bmatrix} u_j \\ W \end{Bmatrix} = [F_j]\{f\} = [F_j][X]\{d\} \quad (16)$$

where F_j is a matrix of order 2×8 which contains the coefficient of displacement component expressed in (16), and $[X]$ is a shape function matrix of order 8×24. The consistent mass matrix of three nodded elements is:

$$[M] = \iiint [X]^T \left([F_j]^T \rho_j [F_j] dz\right)[X] dx.dy \quad (17)$$

Free vibration analysis was performed to determine the fundamental natural frequency from:

$$\left[K_g - \omega^2\{M_g\}\right]\{\lambda\} = 0 \quad (18)$$

where ω is the vibration frequency and λ is the eigenvector. The dynamic response of the composite beam was analyzed using the following equation:

$$[K_g \quad C_g \quad M_g]\begin{bmatrix} d \\ \dot{d} \\ \ddot{d} \end{bmatrix} = \{F_t\} \quad (19)$$

where, d, $\dot{d}$, and $\ddot{d}$ are the displacement, velocity, and acceleration vectors.

III. RESULT AND DISCOUSSION

A C^0 finite element method was used to solve the cubic-order axial displacement equation. These equations were solved using FORTRAN.

A. Comparison Study

To validate the results, the mid-span deflection of a two-layered simply supported composite beam was compared with a T-cross section, using the results of [16], which used the state-step approach to tackle this problem. Table I shows the mid-span deflection of a simply supported composite beam, which varies with its interfacial stiffness. The percentage error mentioned in Table I shows the accuracy of the model.

TABLE I. VARIATION OF MID-SPAN DEFLECTION WITH INTERLAYER SHEAR STIFFNESS.

S.N.	Interfacial shear stiffness (MPa)	Mid-span deflection (mm)	
		Present	[16]
1	10^{-16}	9.7741	9.7224 (0.529)
2	2	8.2072	8.1957 (0.140)

B. Steel-Concrete Porous Beam

This study considered a simply supported composite beam having a porous upper layer. Figure 2 shows the cross-section of the beam. A 15 m long simply supported beam was made up of a porous concrete slab and a steel joist. The dimensions of the concrete slab were 2.25×0.15 m^2. The dimensions of the flange and web of the I-shaped steel joist were 0.1780×013 m^2 and 0.380×0078 m^2, respectively. The material properties of the upper layer were E_c = 13.55 GPa, G_c = 6.775 GPa, and ρ_c = 2396.45 Kg/m^3. Similarly, the material properties of the upper layer were E_s = 200 GPa, G_s = 100 GPa, and ρ_s = 7948.89 Kg/m^3. A 100 KN moving point load is taken for the analysis, moving at a velocity of 16.67 m/s. The interfacial shear stiffness (k_s) of the partially composite beam was considered as 100 MPa.

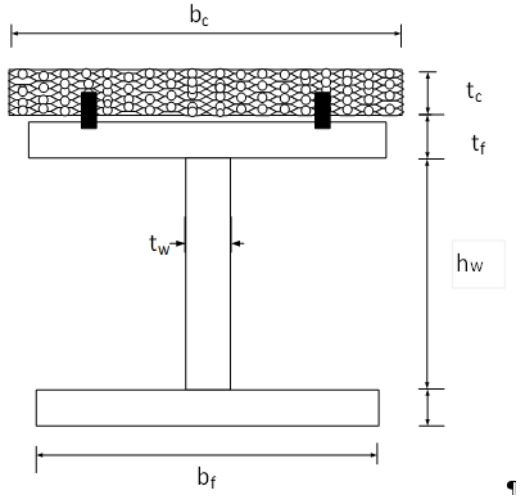

Fig. 2. Cross section of the steel-concrete composite beam.

C. Porosity and Damping Effect on Mid-span Deflection

The porosity of the upper layer ranged from 0 to 0.5. The effect of damping ratios on mid-span deflection was observed. This study used a variation of damping ratios from 0% to 10%. Figures 3 and 4 show that the deflection of the partial and complete composite beams increased with increasing the porosity of the concrete elements.

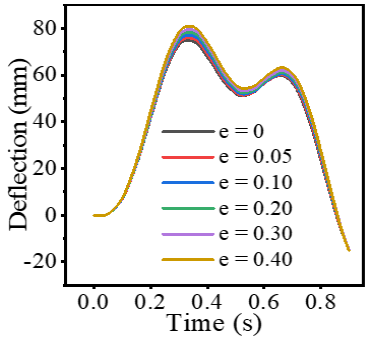

Fig. 3. Variation of deflection with concrete porosity of partial composite beam.

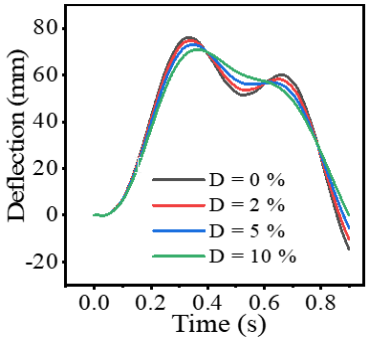

Fig. 5. Variation of deflection of partial composite beam with damping ratio.

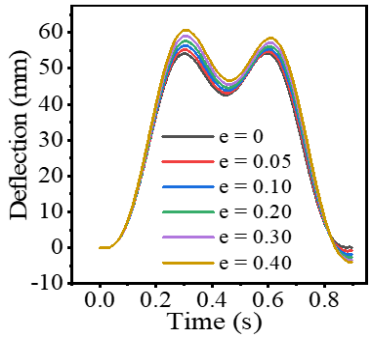

Fig. 4. Variation of deflection with concrete porosity of complete composite beam.

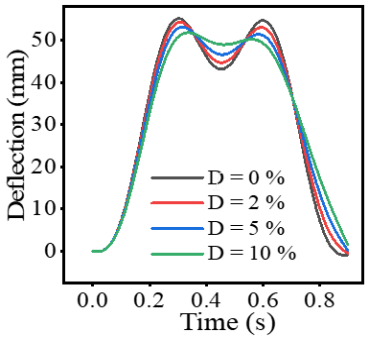

Fig. 6. Variation of deflection of complete composite beam with damping ratio.

TABLE II. VARIATION OF DEFLECTION WITH POROSITY AND DAMPING RATIO.

Porosity (e)	Deflection (mm)							
	Partial Composite				Full Composite			
	D=0%	*D*=2%	*D*=5%	*D*=10%	*D*=0%	*D*=2%	*D*=5%	*D*=10%
0.00	74.789	73.548	71.974	69.931	54.254	53.248	52.138	50.865
0.10	75.898	74.634	73.028	70.936	55.217	54.310	53.170	51.852
0.20	77.043	75.758	74.121	71.982	56.383	55.454	54.284	52.920
0.30	78.239	76.937	75.270	73.085	57.661	56.709	55.506	54.096
0.40	79.512	78.196	76.499	74.269	59.092	58.114	56.877	55.420
0.50	80.898	79.574	77.847	75.573	60.740	59.733	58.457	56.950

The proposed trend of deflection variation satisfied the mathematical formulation above. The magnitude of the material properties of the concrete element decreases with an increase in porosity, and the stiffness of the element was directly proportional to the material properties. Figures 5 and 6 show that the deflection of the partial and complete composite beams decreased with increasing damping ratio, which satisfied the mathematical formulation since the damping effect reduces the load effect. Figures 3-6 show that beam deflection varies when the moving load passes from the left to the right support. Table II satisfies the above pattern of beam deflection.

This study introduced an innovative investigation of the effect of porosity on the bending behavior of a simply supported sandwich composite beam. Porosity in concrete has long been a concern for civil engineers due to its detrimental impact on the strength of concrete elements. In the field of construction, steel-concrete beams are extensively used. Therefore, this study is of significant importance as it provides valuable guidance for future composite material research.

IV. CONCLUSIONS

A C^0 finite element method was used to solve the cubic-order one-dimensional axial displacement equation. The cubic order shear deformation theory was used to analyze the bending behavior of a simply supported composite beam.

- This study took into account the uniform distribution of porosity in the upper layer of the composite, proposing a novel relationship between porosity, damping, and bending.
- The deflection of the simply supported composite beam increased with an increase in the porosity of the upper layer of the partial and complete composite beams.
- The porosity of the upper layer of the composite beam increased from 0.0 to 0.50, and then the beam deflection increased up to 8% in the case of the partial composite and 12% in the case of the complete composite.

- The beam deflection in both the partial and complete composite cases decreased with an increase in damping.
- The beam deflection decreased by 6.5% in the partial composite and 6% in the complete composite, while the damping increased from 0 to 10 %.
- The presented model was more accurate in the prediction of the banding of the composite beam.

ACKNOWLEDGMENT

The authors would like to thank the National Institute of Technology Patna (India) for its financial support.

REFERENCES

[1] D. Mohammed and S. R. Al-Zaidee, "Deflection Reliability Analysis for Composite Steel Bridges," *Engineering, Technology & Applied Science Research*, vol. 12, no. 5, pp. 9155–9159, Oct. 2022, https://doi.org/10.48084/etasr.5146.

[2] K. Swaminathan, D. T. Naveenkumar, A. M. Zenkour, and E. Carrera, "Stress, vibration and buckling analyses of FGM plates—A state-of-the-art review," *Composite Structures*, vol. 120, pp. 10–31, Feb. 2015, https://doi.org/10.1016/j.compstruct.2014.09.070.

[3] A. R. Noori, T. A. Aslan, and B. Temel, "Dynamic Analysis of Functionally Graded Porous Beams Using Complementary Functions Method in the Laplace Domain," *Composite Structures*, vol. 256, Jan. 2021, Art. no. 113094, https://doi.org/10.1016/j.compstruct.2020.113094.

[4] M. G. Taj, A. Chakrabarti, and M. Talha, "Bending analysis of functionally graded skew sandwich plates with through-the thickness displacement variations," *Journal of Sandwich Structures & Materials*, vol. 16, no. 2, pp. 210–248, Mar. 2014, https://doi.org/10.1177/1099636213512499.

[5] H. I. Yoon, I. S. Son, and S. J. Ahn, "Free vibration analysis of Euler-Bernoulli beam with double cracks," *Journal of Mechanical Science and Technology*, vol. 21, no. 3, pp. 476–485, Mar. 2007, https://doi.org/10.1007/BF02916309.

[6] R. Xu and Y. Wu, "Static, dynamic, and buckling analysis of partial interaction composite members using Timoshenko's beam theory," *International Journal of Mechanical Sciences*, vol. 49, no. 10, pp. 1139–1155, Oct. 2007, https://doi.org/10.1016/j.ijmecsci.2007.02.006.

[7] H. Su and J. R. Banerjee, "Development of dynamic stiffness method for free vibration of functionally graded Timoshenko beams," *Computers & Structures*, vol. 147, pp. 107–116, Jan. 2015, https://doi.org/10.1016/j.compstruc.2014.10.001.

[8] A. Chakrabarti, A. H. Sheikh, M. Griffith, and D. J. Oehlers, "Analysis of composite beams with partial shear interactions using a higher order beam theory," *Engineering Structures*, vol. 36, pp. 283–291, Mar. 2012, https://doi.org/10.1016/j.engstruct.2011.12.019.

[9] A. Chakrabarti, A. H. Sheikh, M. Griffith, and D. J. Oehlers, "Dynamic Response of Composite Beams with Partial Shear Interaction Using a Higher-Order Beam Theory," *Journal of Structural Engineering*, vol. 139, no. 1, pp. 47–56, Jan. 2013, https://doi.org/10.1061/(ASCE)ST.1943-541X.0000603.

[10] T. Kant and A. Gupta, "A finite element model for a higher-order shear-deformable beam theory," *Journal of Sound and Vibration*, vol. 125, no. 2, pp. 193–202, Sep. 1988, https://doi.org/10.1016/0022-460X(88)90278-7.

[11] U. A. Girhammar and D. Pan, "Dynamic analysis of composite members with interlayer slip," *International Journal of Solids and Structures*, vol. 30, no. 6, pp. 797–823, Jan. 1993, https://doi.org/10.1016/0020-7683(93)90041-5.

[12] Q.-H. Nguyen, M. Hjiaj, and P. Le Grognec, "Analytical approach for free vibration analysis of two-layer Timoshenko beams with interlayer slip," *Journal of Sound and Vibration*, vol. 331, no. 12, pp. 2949–2961, Jun. 2012, https://doi.org/10.1016/j.jsv.2012.01.034.

[13] M. H. Yas and M. Heshmati, "Dynamic analysis of functionally graded nanocomposite beams reinforced by randomly oriented carbon nanotube under the action of moving load," *Applied Mathematical Modelling*, vol. 36, no. 4, pp. 1371–1394, Apr. 2012, https://doi.org/10.1016/j.apm.2011.08.037.

[14] A. K. Gupta and A. Kumar, "Buckling Analysis of Porous Functionally Graded Plates," *Engineering, Technology & Applied Science Research*, vol. 13, no. 3, pp. 10901–10905, Jun. 2023, https://doi.org/10.48084/etasr.5943.

[15] P. Kumar and A. Kumar, "Free Vibration Analysis of Steel-Concrete Pervious Beams," *Engineering, Technology & Applied Science Research*, vol. 13, no. 3, pp. 10843–10848, Jun. 2023, https://doi.org/10.48084/etasr.5913.

[16] X. Shen, W. Chen, Y. Wu, and R. Xu, "Dynamic analysis of partial-interaction composite beams," *Composites Science and Technology*, vol. 71, no. 10, pp. 1286–1294, Jul. 2011, https://doi.org/10.1016/j.compscitech.2011.04.013.